PHYSICAL REVIEW D **79,** 034012 (2009)

Phase conversion in a weakly first-order quark-hadron transition

A. Bessa,[1,*] E. S. Fraga,[2,†] and B. W. Mintz[2,‡]

[1]*Instituto de Física, Universidade de São Paulo, Caixa Postal 66318, 05315-970, São Paulo, SP, Brazil*
[2]*Instituto de Física, Universidade Federal do Rio de Janeiro, Caixa Postal 68528, 21941-972 Rio de Janeiro, RJ, Brazil*
(Received 6 December 2008; published 12 February 2009)

We investigate the process of phase conversion in a thermally driven *weakly* first-order quark-hadron transition. This scenario is physically appealing even if the nature of this transition in equilibrium proves to be a smooth crossover for vanishing baryonic chemical potential. We construct an effective potential by combining the equation of state obtained within lattice QCD for the partonic sector with that of a gas of resonances in the hadronic phase, and present numerical results on bubble profiles, nucleation rates, and time evolution, including the effects from reheating on the dynamics for different expansion scenarios. Our findings confirm the standard picture of a cosmological first-order transition, in which the process of phase conversion is entirely dominated by nucleation, also in the case of a weakly first-order transition. On the other hand, we show that, even for expansion rates much lower than those expected in high-energy heavy-ion collisions, nucleation is very unlikely, indicating that the main mechanism of phase conversion is spinodal decomposition. Our results are compared to those obtained for a strongly first-order transition, as the one provided by the MIT bag model.

DOI: 10.1103/PhysRevD.79.034012 PACS numbers: 25.75.Nq, 64.60.Q−, 64.75.−g

I. INTRODUCTION

It is widely accepted that experiments in high-energy heavy-ion collisions at the Relativistic Heavy Ion Collider (RHIC) have produced clear signals that nuclear matter undergoes a phase transition to a deconfined partonic phase at sufficiently large values of energy density [1,2]. A similar transition presumably took place in the early universe a few seconds after the big bang [3,4]. In fact, this whole picture is expected from quantum chromodynamics (QCD), which exhibits the phenomenon of asymptotic freedom. The nature of the quark-hadron transition, nevertheless, remains an open question. Although lattice QCD [5], whose recently improved techniques allow for performing calculations with almost realistic quark masses [6], seems to indicate a crossover, the possibility of a weakly first-order transition is not ruled out from the experimental point of view. In reality, most hydrodynamic calculations within high-energy heavy-ion collisions adopt an equation of state which provides a strongly first-order transition [1].

Another point that is seldom mentioned is that, being built on equilibrium assumptions, lattice QCD thermodynamics does not provide any information on the dynamical nature of the deconfining transition. In actual experiments, the critical (dynamical) behavior could be very different from what one would expect from a crossover in the (equilibrium) phase diagram, simply because the phase conversion is achieved via a nonequilibrium evolution process [7,8]. Indeed, results from simulations in statistical mechanics show that the critical behavior can differ significantly if one compares the equilibrium phase diagram to the (nonequilibrium) time evolution of a given system, and suggest that the dynamics could change the nature of the phase transition, even though the situation is still unclear [9,10]. For these reasons, the scenario of a *weakly* first-order deconfining transition is physically appealing, especially since it comes out naturally by matching two equations of state that are realistic in their own regimes of temperature, namely, the equations of state provided by lattice QCD and by a hadron resonance gas.

In this paper we investigate the process of phase conversion in a thermally driven *weakly* first-order quark-hadron transition. We build an effective potential by combining the equation of state obtained from lattice simulations for one heavy and two light flavors of quarks, which we use for the partonic sector, with the equation of state of a gas of resonances for the hadronic phase. Using standard techniques for the dynamics of first-order transitions, we compute bubble nucleation features, such as bubble profiles, critical radii, the surface tension, and the free energy as functions of the temperature. We study the process of phase conversion evaluating the nucleation rate and investigating the time evolution of the temperature of the system and its hadronic fraction, as well as the role played by reheating.

Bubble nucleation is one of different simplified mechanisms used to describe the dynamics of a first-order phase transition [8]. In this kind of transition, for temperatures slightly lower than the critical temperature, T_c, the thermodynamic potential exhibits a metastable minimum besides the global minimum. The former gradually disappears as the system cools down, and is turned into a point of inflection known as spinodal instability. By de-

*abessa@if.usp.br
†fraga@if.ufrj.br
‡mintz@if.ufrj.br

creasing further the temperature, the transition follows a qualitatively different (explosive) evolution, since the free energy barrier disappears and there is no extra surface cost for small amplitude long-wavelength fluctuations. Therefore, depending on the dynamics of supercooling, the phase conversion can proceed via more than one mechanism. In a slowly expanding system, the phase transition occurs through the nucleation of bubbles of the ''true vacuum'' state via thermal activation. In general, in order to know whether the system reaches the spinodal instability before nucleation is completed, it is necessary to investigate the time scale for thermal nucleation relative to that for the expansion. In the case of the quark-gluon plasma (QGP) presumably formed in ultrarelativistic heavy-ion collisions, the expansion of the plasma is faster than that in the case of the early universe during the cosmological quark-hadron transition by a factor of $\sim 10^{18}$. Thus, it is clear that one should expect major differences in the process of phase conversion when comparing the big bang to the little bang [11].

Our findings confirm the standard picture of a cosmological first-order transition, in which the process of phase conversion is entirely dominated by nucleation, also for the case of a weakly first-order transition. On the other hand, we show that, even for expansion rates much lower than those expected in high-energy heavy-ion collisions, nucleation is very unlikely, indicating that the main mechanism of phase conversion is spinodal decomposition. Our results are compared to those obtained for a strongly first-order transition, as the one provided by the MIT bag model.

The dynamics of nucleation and spinodal decomposition in the hadronization of an expanding QGP after a high-energy heavy-ion collision has been studied under different approaches for more than 20 years [12–22], as is also the case for the cosmological quark-hadron transition [23,24]. However, previous studies were mostly based on equations of state obtained in the frame of the MIT bag model or within effective models, such as the linear sigma model [25], the Nambu-Jona-Lasinio model [26], and the Polyakov loop model [27] in the environment of a strongly first-order transition. Only more recently, stimulated by the findings of lattice QCD, a few studies have considered the case of a smooth crossover, and how its dynamics compares to a strongly first-order transition, including the effects from fluctuations and inhomogeneities and the presence of a critical point [28–30]. Our proposal in this paper is, as described above, to investigate a scenario which is in between these two extrema. Furthermore, in the case of high-energy heavy-ion collisions, in which there is a very fast quench down to the spinodal instability, the dynamics can possibly be well described by spinodal decomposition even in the case of a smooth (but very fast) crossover.

The paper is organized as follows. Section II reviews the theoretical methods we use to describe the nucleation process of an expanding system, including a brief presentation of the thin-wall approximation following a different reasoning, and discusses the dynamics in an expanding background plus the role of reheating. Our numerical results are discussed in Sec. III, where we display the relevant bubble features, as well as the time evolution of the temperature and of the hadronic fraction, and analyze the process of reheating. Finally, our conclusions are presented in Sec. IV.

II. THEORETICAL FRAMEWORK

Thermodynamically, a phase transition happens when a given system shifts its state of equilibrium from one free energy minimum to another in response to the change of some critical thermodynamic parameter. In real transitions, this shift between equilibrium states is often an essentially nonequilibrium process and, in principle, one has no hope to describe it using the machinery of equilibrium thermodynamics. However, several natural systems exhibit phase transitions in which the system is trapped in a metastable state (false vacuum) for a long time before reaching the final equilibrium configuration (true vacuum). This is certainly true in a strongly first-order scenario in which the time scale of supercooling (superheating) in a thermally driven transition is not much faster than the typical reaction time of the system. A first-order phase transition occurs between noncontiguous states in the thermodynamic configuration space, and manifests itself as a discontinuity in the entropy. This latent heat is a consequence of an energy barrier that prevents the system to simply roll down to the true minimum. If this barrier is high (characteristic of a strongly first-order transition), a statistically improbable fluctuation is required, and the system is held in a metastable state for an appreciable time interval.

A similar metastable behavior sets in when the change in the critical parameter is fast as compared to the relaxation time of the system. This is the case of the hadronization of the QGP formed in high-energy heavy-ion collisions, where the time scale of the expanding plasma is orders of magnitude shorter than the typical reaction time of the deconfined matter. It turns out that it can be impossible (and immaterial) to determine the ''real nature'' of the phase transition in this dynamical system since the quenched plasma does not have to follow a continuous path in the thermodynamic configuration space. Assuming a weakly first-order scenario for the quark-hadron transition, we review in the next sections some theoretical tools used in the description of the decay of metastable states.

A. Homogeneous nucleation

The paramount example of metastability in a first-order transition is the supersaturated vapor in a gas-liquid mixture below the condensation temperature. The mixture is composed of bubbles of liquid suspended in the gas, the

two phases separated by a definite surface. Taking into account the surface energy of the partially developed phase, the notion of thermodynamic equilibrium can be extended in spite of the fact that the gas cannot be in equilibrium with a fully developed liquid phase. Since it takes energy to make a surface, small bubbles will not be energetically favorable, and will be constantly created and evaporated. On the other hand, if a sufficiently large bubble is formed in the medium, it will tend to grow, eventually converting the entire system to the new phase.

The mechanism of bubble nucleation can play an important role in a first-order phase transition. It ignores the initial stages of the development of bubbles, being an effective theory for semimacroscopic elements of volume. Still, one may have a flavor of what really happens by studying the dynamics of the nucleated bubbles. The question of the formation of bubbles is extremely relevant, mainly when external agents play the role of nucleating centers, leading to a significant increase of the nucleation rate. This is actually what happens to most natural systems, and is known as heterogeneous nucleation. However, we will not consider this kind of nucleation mechanism, but one in which bubbles originate from intrinsic thermodynamic fluctuations: the mechanism of homogeneous nucleation. It is a more fundamental process for which there is a field theory which captures its basic features. Most of the formalism is based on a series of papers written by Langer in the late sixties [31], where the basic theoretical apparatus to describe the decay of a metastable state of a classical system interacting with a heat bath at temperature T is proposed (see also [32]). In this approach, stable and metastable phases appear as local minima of a smooth energy functional E. Based on a phenomenological droplet model, it is conjectured that, in going from one minimum to a neighbor one, the system is likely to pass across a saddle point which is a minimum of E in all directions of functional space but one, the latter giving rise to the instability. This saddle-point configuration plays the role of the critical bubble in the formalism. Langer derived an equation of motion for the probability distribution of the system, and obtained a steady-state solution flowing across the saddle point, allowing for the calculation of a classical nucleation rate (probability per unit time per unit volume that a critical bubble nucleates)

$$\Gamma = \frac{|\lambda_{-1}|}{\pi T} \mathrm{Im} F, \tag{1}$$

where F is a prescribed analytic continuation of the free energy of the stable phase in the unbroken (single-well) version of the theory which becomes metastable after the analytic continuation. The parameter λ_{-1} is the negative eigenvalue of the fluctuation operator characterizing the instability of the saddle-point configuration.

The zero-temperature quantum field theoretic case, where transitions are exclusively due to quantum tunneling, was considered by Coleman and Callan in [33], and, when both quantum and thermal fluctuations act together, the decay rate is approximately given by (1), as proved by Affleck [34] in a quantum mechanical context. Of course, the existence of a single direction of instability simplifies the extension of Langer's formalism to quantum field theories, and direct applications were proposed in the literature [35,36].

A good description of the nucleation process relies on a suitable choice of the free energy functional governing the dynamics of the bubbles. The natural choice corresponds to deriving the free energy from a more fundamental theory. When this is not feasible, and this is the case for the full QCD Lagrangian, one can resort to a phenomenological approach, imposing symmetry requirements, as will be discussed in the next section.

B. Effective potential and equations of state

As customary, one can obtain information about the phase transition by studying the evolution of a scalar field ϕ which represents the order parameter. It is reasonable to assume spherical symmetry for nucleating bubbles, so that one defines a coarse-grained free energy functional of the form:

$$F(\phi) = 4\pi \int r^2 dr \left[\frac{1}{2} \left(\frac{d\phi}{dr} \right)^2 + V(\phi) \right]. \tag{2}$$

Thus, the field ϕ evolves in space in the presence of an effective potential that can be parametrized in the form of a Landau expansion around the equilibrium phases, i.e.

$$V(\phi) = a(T)\phi^2 - bT\phi^3 + c\phi^4. \tag{3}$$

The parameters $b > 0$, $c > 0$, and $a(T)$, and the interpretation of the order parameter are determined by the scenario under consideration, namely, the supercooled ($T < T_c$) QGP. One should notice that, in this simple approach, the temperature enters only as a parameter of the effective potential.

The potential (3) is suitable for a first-order phase transition due to the properties of its extrema. The order parameter configurations (bubble profiles) are solutions of the following Euler-Lagrange equation:

$$\frac{d^2\phi}{dr^2} + \frac{2}{r}\frac{d\phi}{dr} - V'(\phi) = 0. \tag{4}$$

The potential (3) has two minima, ϕ_q and ϕ_h, which correspond to the equilibrium phases. Here, ϕ_q (ϕ_h) corresponds to the quark (hadron) phase. There is a barrier separating ϕ_q and ϕ_h which can be associated with a latent heat, a jump in entropy from one phase to the other. In addition, one can prove that, as required by Langer's formalism, this theory has a saddle-point solution, ϕ_b, connecting the two minima and with a single unstable direction [31]. The minimum ϕ_q is conveniently chosen to be zero, while the other one is located at

$$\phi_h = \frac{1}{8c}(3bT + \sqrt{9b^2T^2 - 32a(T)c}). \quad (5)$$

The transition temperature is reached when the pressures of the competing phases coincide. This condition sets a connection with thermodynamics through the identification

$$p_q(T) - p_h(T) = V(\phi_h, T); \qquad V(\phi_q, T) = 0, \quad (6)$$

where p_q and p_h are the pressures of the quark (deconfined) phase and hadron phase, respectively.

In order to proceed with the study of the phase conversion from the deconfined state to hadrons, one has to fix the potential, either by connecting it to pressures computed for each phase, as described above, or by extracting the effective potential directly from some effective field theory, such as the linear sigma model as, for instance, in Refs. [20,28]. We choose to follow the first procedure and, instead of using the MIT bag model as usually done for simplicity, we profit from the currently more robust knowledge of the equation of state of QCD in the two different regimes (partonic and hadronic) which justifies the use of more realistic expressions for the pressure. Concretely, we use lattice QCD results for $N_f = 2 + 1$ quark flavors to describe the high-temperature sector [37], and a gas of over 250 free resonances for the hadronic phase [38]. This yields a *weakly* first-order deconfining transition, to be contrasted to the usual case of a strongly first-order transition as provided by the bag model, and the value of the critical temperature is automatically determined by the crossing of the high and low temperature pieces of the equation of state (EoS), as illustrated in Fig. 1. For comparison, we also use the bag model for the quark phase in our calculations and discussion, choosing the bag constant according to the critical temperature obtained by the crossing of the pressure curves [39].

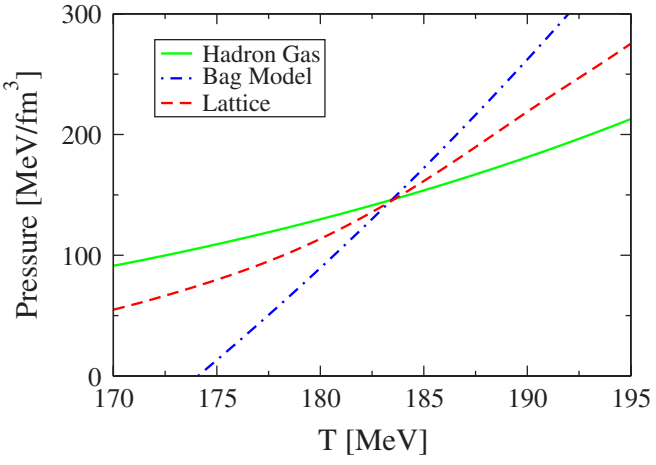

FIG. 1 (color online). Pressures for the hadron resonance gas (solid line), bag model (dash-dotted line), and $N_f = 2 + 1$ lattice QCD (dashed line) equations of state.

Finally, the relations (6) leave two remaining conditions to be imposed on the potential. These can be chosen to fit a pair of physical properties of the critical bubble near the transition temperature, such as the surface tension and the correlation length [13].

C. The thin-wall approximation revisited

It is always convenient to consider the following auxiliary mechanical problem in the solution of Eq. (4): the one-dimensional dynamics of a particle moving in a dissipative medium in the presence of the potential $(-V)$. Ignoring the dissipative term, strictly at $T = T_c$, the solution of Eq. (4) can be written in terms of elementary functions. The aim of this section is to discuss approximate analytic solutions for temperatures close (in some precise sense) to T_c, where dissipation must be present.

In order to explore this case, it is convenient to write the potential V as the sum of the critical potential plus a linear term which introduces deviations from $T = T_c$ [20]. This is always possible for a quartic potential up to a shift in the zero of the energy. In the present case, we obtain $V(\phi) = W(\phi + \mu) + W_0$, where W_0 is a constant,

$$W(\phi) = c(\phi^2 - \phi_0^2)^2 + j\phi, \quad (7)$$

$$\phi_0^2 = \frac{1}{2}\left[\frac{3}{8}\left(\frac{bT}{c}\right)^2 - \frac{a(T)}{c}\right], \quad (8)$$

$$j = \frac{c}{2}\left[\frac{a(T)bT}{c^2} - \frac{1}{4}\left(\frac{bT}{c}\right)^3\right], \quad (9)$$

and $\mu = -bT/4c$. The corresponding Euler-Lagrange equation has the same form as (4), with W' replacing V'. The critical $(T = T_c)$ potential (for which $j = 0$) is a symmetric double well with minima at $\phi = \pm\phi_0$. In terms of these parameters, the solution in the thin-wall approximation at $T = T_c$ is a kink which interpolates between the two symmetric minima:

$$\phi_b(r) = \phi_0 \tanh\left(\frac{r - R}{\xi}\right), \quad (10)$$

where $\xi = 1/(\phi_0\sqrt{2c})$ can be thought of as a correlation length. When dissipation is neglected, the previous function is a solution for any value of R. Given the specific form of the dissipation term, approximate solutions for the full potential are obtained for large values of R/ξ. The limit $\xi/R \ll 1$ characterizes the so-called thin-wall regime [8].

For $T < T_c$, the parameter j is negative and the two minima of W are shifted to

$$\phi_f = \mu \approx -\phi_0\left(1 + \frac{j}{8c\phi_0^3}\right) \quad (11)$$

and

$$\phi_t = -\frac{1}{2}\mu + \frac{1}{2}\sqrt{4\phi_0^2 - 3\mu^2} \approx \phi_0\left(1 - \frac{j}{8c\phi_0^3}\right). \quad (12)$$

When $|j/(8c\phi_0^3)| \ll 1$, the potential is only slightly tilted. In this range, the dissipation term will be small, and it is reasonable to assume that the interpolating solution still has a kinklike profile, i.e.,

$$\phi_b(r) = \phi_f + \frac{\phi_t - \phi_f}{2}\left[1 - \tanh\left(\frac{r-R}{\xi}\right)\right], \tag{13}$$

where $\xi = \sqrt{2/c}(\phi_t - \phi_f)^{-1}$. Still in this limit, one can show that the free energy of the bubble ϕ_b is given by

$$F(\phi_b) = -\frac{4\pi R^3}{3}\Delta W + 4\pi R^2\sigma, \tag{14}$$

where $\Delta W = W(\phi_f) - W(\phi_t) \approx 2a|j|$, and the surface tension, σ, is related to the parameters of the problem through

$$\sigma \equiv \int_0^\infty \left(\frac{d\phi_b}{dr}\right)^2 dr \approx \frac{2}{3c\xi^3}. \tag{15}$$

As discussed in the previous subsection, the value of σ at $T = T_c$ and the constant value of ξ will be considered as inputs in our treatment. In terms of these quantities, the coefficients of the potential (3) are completely determined. Imposing that ϕ_b be stationary, we obtain the critical radius

$$R_c = \frac{2\sigma}{\Delta W}. \tag{16}$$

Strictly speaking, the function (13) is an exact solution only at $T = T_c$, where $j = 0$ and R_c diverges. A different approach consists in taking the dissipation into account in the following manner: (i) the solution conserves energy; (ii) it is exact at T_c. We can impose both conditions to a function of the form

$$\psi_b(r) = \phi_f + \gamma\left[1 - \tanh\left(\frac{r-\tilde{R}_c}{\tilde{\xi}}\right)\right]. \tag{17}$$

Condition (ii) gives

$$\tilde{R}_c = \frac{2\gamma/\tilde{\xi}}{-j + 4c(\mu+\gamma)[\phi_0^2 - (\mu+\gamma)^2]}, \tag{18}$$

whereas condition (i) is equivalent to

$$\int_0^\infty \frac{2}{r}\left(\frac{d\psi_b(r)}{dr}\right)^2 dr = W(\phi_f) - W(\psi_b(0)). \tag{19}$$

In the thin-wall limit ($\tilde{\xi}/\tilde{R}_c \ll 1$), condition (i) is simply

$$\frac{8\gamma^2}{3\tilde{\xi}\tilde{R}_c} = W(\phi_f) - W(\phi_f + 2\gamma). \tag{20}$$

Coupling (i) with (ii) leads to $\gamma = (\phi_v - \phi_f)/2$, $\tilde{\xi} = \xi$, and $\tilde{R}_c = R_c$. Numerical results point to a kinklike solution with a decreasing escape value when one decreases the temperature. This fact explains the behavior of the surface tension plotted in Fig. 4 within this approximation.

Once we have an (approximated) expression for the bubble solution, we can use it to calculate the decay rate shown in Eq. (1). This rate can be written as [31]

$$\Gamma = \frac{\mathcal{P}_0}{(2\pi)} e^{-\Delta F/T}, \tag{21}$$

where ΔF is the difference in free energy between the saddle-point configuration (ϕ_b) and the metastable phase (ϕ_f). The prefactor $\mathcal{P}_0$ is a product of a dynamical factor κ (related to the expansion rate of the bubbles) and a statistical factor Ω_0, which accounts for the first corrections to ΔF due to quadratic fluctuations around each extremum. As usual, these quadratic fluctuations are formally written in terms of the determinant of the fluctuation operator $[\nabla^2 - V''(\phi)]$, where ϕ is either ϕ_f or ϕ_b. Thus, one obtains

$$\Omega_0 = (\pi R_c^2 T)^{1/2}\left(\frac{4\pi R_c^2\sigma}{3}\right)^{3/2}\left\{\frac{\det'[\nabla^2 - V''(\phi_b)]}{\det[\nabla^2 - V''(\phi_f)]}\right\}^{-1/2}, \tag{22}$$

where the prime indicates that the zero and negative modes are excluded. The first term in the (right-hand side) r.h.s. of (22) comes from the negative eigenvalue of the fluctuation operator along the direction of instability. The second term is the contribution from the three zero modes which are present because the bubble breaks translational symmetry. Except for the four unpaired eigenvalues of $[\nabla^2 - V''(\phi_f)]$, all the other delocalized eigenvalues of that operator cancel the corresponding ones of $[\nabla^2 - V''(\phi_b)]$. Taking all the remaining contributions into account, it is possible to show that [35]

$$\Omega_0 = \frac{2}{3\sqrt{3}}\left(\frac{\sigma}{T}\right)^{3/2}\left(\frac{R_c}{\xi_q}\right)^4, \tag{23}$$

where ξ_q is identified as the correlation length of the metastable phase. For the dynamical coefficient, Csernai and Kapusta derived the following expression [13]:

$$\kappa = \frac{4\sigma(\zeta + 4\eta/3)}{(\Delta\omega)^2 R_c^3}. \tag{24}$$

In the previous formula, ζ and η are, respectively, the bulk and shear viscosity coefficients of the quark phase, and $\Delta\omega$ is difference in the enthalpy density of quark and hadron phases (see also Ref. [40] for a careful discussion of the dynamical prefactor).

D. Dynamics of the phase conversion in an expanding background

As soon as a QGP is formed after a high-energy collision of heavy ions or in the early universe, it expands towards the empty space around it. Because of this expansion, the energy density and, therefore, the temperature of the plasma drops and eventually becomes smaller than the critical temperature for the quark-hadron phase transition.

Assuming a weakly first-order transition, as discussed before, the system then becomes metastable and the nucleation of bubbles of the cold phase is possible. If the expansion rate is large enough, however, the system supercools so fast that it may reach a thermodynamically unstable region of the phase diagram, the spinodal region, before nucleation is able to drive most of the system to the true vacuum. In this case, the phase conversion is dominated by the process of spinodal decomposition, which is rather different from nucleation, since it is characterized by long-ranged fluctuations, instead of localized nucleating bubbles [8]. Here we focus on the nucleation stage during the expansion, and how the nucleation and expansion time scales compare.

For simplicity, we consider a homogeneous and isotropic expansion of the fluid, and assume that the Hubble parameter $H(x) \equiv \partial_\mu u^\mu(x)$ is actually a constant. We also assume that the entropy is approximately conserved (globally) during the expansion, once the viscosity of the QGP is very low, as indicated by heavy-ion collision experiments [2,41]. However, the viscosity cannot be strictly zero, once it is necessary for the process of nucleation at vanishing chemical potential (see, e.g., Ref. [40]). For definiteness, we assume that the viscosity coefficient in Eq. (24), $\zeta + 4\eta/3$, is of the order of the lower bound set by holographic models [42].

To have a measure of the importance of nucleation in the hadronization process, we estimate how much of an expanding plasma should hadronize through nucleation before the spinodal temperature is reached. In a first approach, we employ some simplifying assumptions. The first of them is to neglect reheating effects (which will be considered later) and, assuming the conservation of entropy:

$$\frac{d}{dt}(sa^3) = 0. \tag{25}$$

The assumption of isotropic expansion leads to the Hubble law for the scale factor $a(t)$,

$$\frac{da}{dt}(t) = Ha(t), \tag{26}$$

and Eq. (26) leads to an exponential decay of the temperature with time

$$T(t) = T_c \exp(-Ht), \tag{27}$$

where $t = 0$ is chosen to correspond to $T = T_c$.

Given an equation of state and an effective potential, we can find the spinodal temperature of the system, $T_{\rm sp}$, and the time $t_{\rm sp}$ the plasma takes to reach this temperature. For our equation of state, $T_{\rm sp}/T_c = 0.984$, which leads to $Ht_{\rm sp} \sim 0.01$. The fraction $f(t)$ of space which suffers nucleation from $t(T_c) \equiv 0$ until $t_{\rm sp} \equiv t(T_{\rm sp})$ can be *overestimated* as follows:

$$f(t_{\rm sp}) = \int_0^{t_{\rm sp}} dt \frac{4\pi}{3} R^3(t, t_{\rm sp}) \Gamma[T(t)] < \frac{4\pi}{3}(t_{\rm sp} T_c)^4 \sim 10^{-3} \ll 1, \tag{28}$$

where $R(t', t)$ is the radius at time t of a bubble "born" at time t' [$R(t', t) < c(t - t')$]. In this estimate we also use the value $H^{-1} = 10$ fm/c, which should also give an extra overestimating contribution to $f(t_{\rm sp})$.[1] We see that, if we neglect reheating effects, typical QGP expansion times in heavy-ion collisions rule out nucleation and therefore most of the plasma should hadronize via spinodal decomposition, a result that was also obtained using the linear sigma model [16,20].

However, once a bubble of the true vacuum is nucleated, an amount of latent heat proportional to the volume of the bubble is released in the medium, so that the temperature does not fall exponentially as in the previous case. If the nucleation rate is high enough, the released latent heat may win the competition against the energy loss due to the fluid expansion and the plasma reheats. This reheating can drive the system to temperatures close to T_c, decreasing the supercooling rate and considerably delaying its arrival at the spinodal temperature. In this case, when we may say that reheating is effective, the whole system is hadronized via nucleation of bubbles and $T_{\rm sp}$ will be reached only some time after the transition is completed.

E. Reheating

In order to account for reheating effects, we make some assumptions aside from those cited on the previous sections. First, the latent heat released in the formation of a true vacuum bubble is uniformly distributed throughout the whole plasma, which is consistent with that of bubble growth via weak deflagration [23]. Therefore, if $s_q(T)$ ($s_h(T)$) is the entropy in the QGP (hadron gas) phase and $s(T)$ is the space average of the entropy density,

$$s = s_h f + (1 - f) s_q, \tag{29}$$

then entropy conservation implies

$$s = \left(\frac{a(0)}{a(t)}\right)^3 s_q(T_c), \tag{30}$$

where we set $T = T_c$ and $s = s_q$ at $t = 0$. For a supercooling $\delta \equiv (T_c - T)/(T_c - T_{\rm sp}) \ll 1$, we have $s_q(T) \approx s_q(T_c)$ and using the thermodynamic relation $-p = \Delta V = e - Ts$, we find a relation between the temperature and the scale factor at a given time t:

$$\left(\frac{T(t)}{T_c}\right)^3 = \left(\frac{a(0)}{a(t)}\right)^3 + f\frac{\Delta s(T)}{s_q(T_c)}, \tag{31}$$

[1] H^{-1} is usually estimated to be in the range 1–10 fm/c for the expanding QGP created in heavy-ion collisions [43].

where $\Delta s(T) = s_q(T) - s_h(T)$ is proportional to the latent heat ℓ at $T \approx T_c$. Once we consider a constant Hubble parameter H, the scale factor grows exponentially, $a(t) = a(0)e^{Ht}$, and Eq. (31) becomes an implicit equation for the temperature as a function of time. We see that the first term on the r.h.s. of Eq. (31) accounts for the cooling due to the expansion, while the second is proportional to the hadronized fraction f and reflects the homogeneous reheating caused by the phase conversion.

We compute f using the expression [44]

$$f(t) = 1 - \exp\left\{-\int_0^t dt' \left(\frac{a(t')}{a(t)}\right)^3 \Gamma[T(t')] \frac{4\pi}{3} R^3(t', t)\right\}, \tag{32}$$

where $R(t', t)$ is the radius of a bubble created at time t' with critical size $R_c[T(t')]$ at time t:

$$R(t', t) = R_c[T(t')] \frac{a(t)}{a(t')} + \int_{t'}^t dt'' v_w[T(t'')] \frac{a(t)}{a(t'')}. \tag{33}$$

We suppose that the velocity of the bubble wall at the temperature T is given by the following Allen-Cahn equation, which relates the velocity of a domain wall to the local curvature [8,45]:

$$v_w(T) = \frac{\Delta p(T)}{\eta} = -\frac{\Delta V(T)}{\eta}, \tag{34}$$

where $\Delta p(T) = -\Delta V(T) \equiv V_q(T) - V_h(T) > 0$ is the pressure difference between the two phases at a given temperature T. This expression corresponds to a steady growth of the bubble in which the pressure difference between both sides of the bubble wall is balanced by a damping force which is proportional to the velocity of the wall. The friction coefficient η is given by

$$\eta = \tilde{\eta} T \sigma(T), \tag{35}$$

where

$$\sigma(T) = \int_0^\infty dr \left(\frac{d\phi}{dr}\right)^2 \tag{36}$$

is the surface tension as a function of the temperature, and $\tilde{\eta}$ is a number of order one.

We solve the set of equations (31)–(34) numerically, and the results are presented in the following section.

III. RESULTS AND DISCUSSION

A. Bubble features

In what follows, we calculate the main physical attributes of critical bubbles both numerically and using the thin-wall approximation. Figure 2 shows bubble profiles, $\Phi(r)$, for various temperatures. It is clear that the numerical results and the thin-wall approximation give very similar results for temperatures close to T_c and become more and more different as the temperature is lowered, as expected. One of the main differences is the broadening of the numerical profile, which does not happen with the thin-wall result, indicating not only the failure of this approximation for lower temperatures but also the failure of the nucleation picture itself as the system approaches the spinodal temperature.

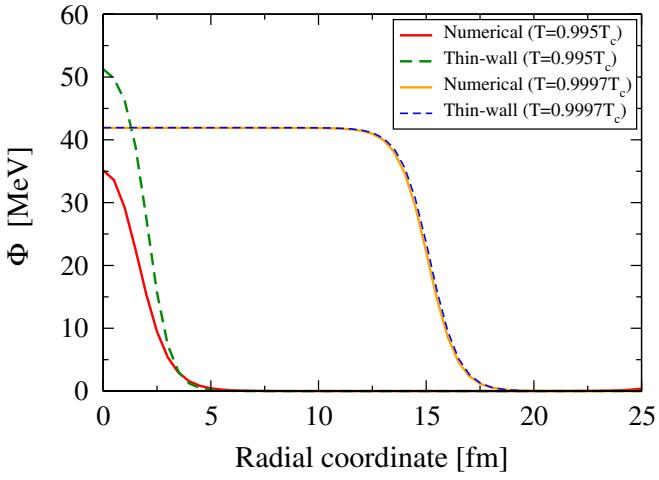

FIG. 2 (color online). Order parameter distributions (bubble profiles), where the broken (hadronic) phase is inside the bubble ($r < R_c$) and the unbroken (QGP) outside ($r > R_c$).

From the bubble profiles we obtain two important quantities: the bubble critical radius and the surface tension. The critical radius as a function of the temperature is shown in Fig. 3. Notice that the critical radius (defined here as the distance from the bubble center in which $\phi = \phi_0/2$) diverges at the critical temperature, as seen in Sec. II C, and also diverges at the spinodal temperature. Notice, however, that for these high values of supercooling, the very concept of a bubble does not make sense any longer, once the width of the wall is larger than the bubble radius.

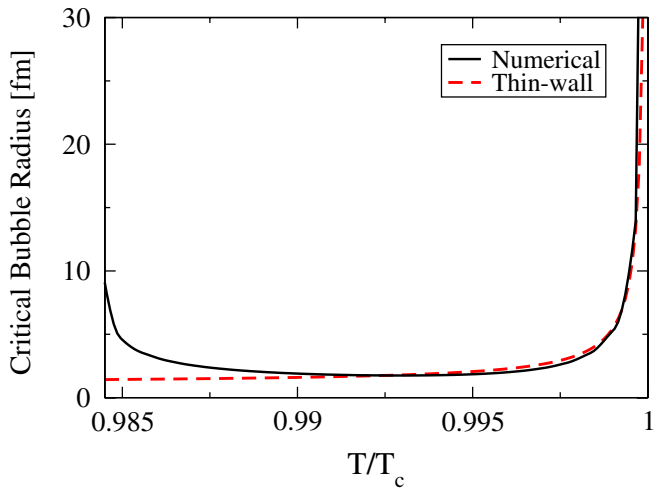

FIG. 3 (color online). Radius of the critical bubble as a function of T/T_c.

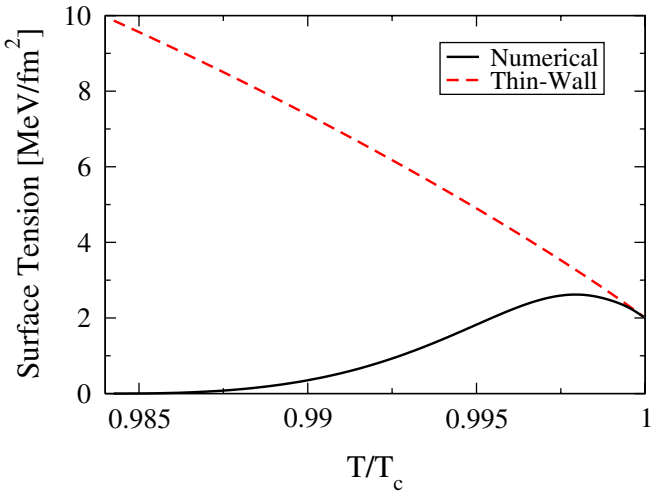

FIG. 4 (color online). Surface tension as a function of T/T_c.

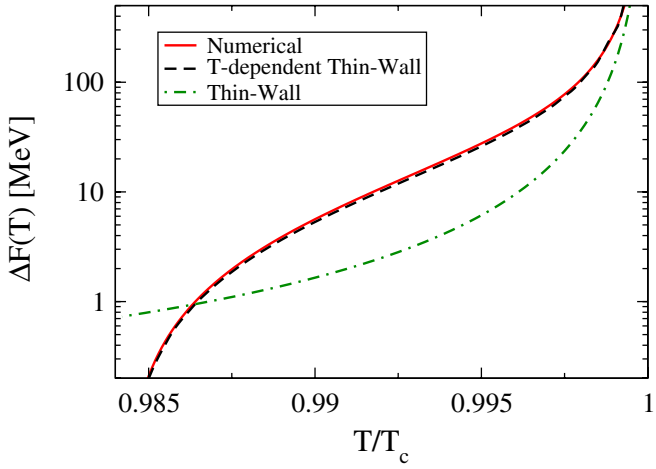

FIG. 5 (color online). Change in free energy, ΔF, calculated in three different ways (see text for details). The thin-wall approximation leads to an *overestimate* of the nucleation rate.

The surface tension, $\sigma(T)$, exhibits an interesting behavior, as displayed in Fig. 4. From its value at $T = T_c$, $\sigma(T_c) = 2$ MeV/fm^2, downwards it starts to grow up to a maximum value and then decreases from this point down. Roughly speaking, the value of the surface tension is the slope $p(r) \equiv (d\phi/dr)^2$ times the width of the wall $\xi(T)$, i.e., the region in which $p(r) \neq 0$. As the temperature is lowered from T_c, the wall is progressively broadened, but $p(r)$ does not change much. As a consequence, the surface tension increases. It is only when $p(r)$ starts to decrease faster than the increase of $\xi(T)$ that $\sigma(T)$ decreases too. This happens for lower temperatures because the order parameter deep into the bubble, $\phi(r = 0)$, becomes smaller, as can be seen in Fig. 2 and, therefore, $p(r)$ also becomes smaller. Notice that the thin-wall approximation is not very sensitive to this competition between the width of the wall and the discontinuity of the order parameter across it because its bubble profiles always connect the two minima, having $\phi_h(T)$ as the decisive parameter, which decreases more slowly than the exact (numeric) $\phi(r = 0)$ for lower temperatures. Therefore, in the thin-wall approximation, $\sigma(T)$ is a monotonically decreasing function of T. This nontrivial behavior of $\sigma(T)$ suggests that the temperature in which $\sigma(T)$ reaches its maximum can be interpreted as a (generous) limit to the applicability of the thin-wall approximation. Following the previous criterion, one can say that the thin-wall approximation fails for supercooling higher than $\delta = 0.1$.

Our aim in calculating all these quantities is to evaluate the change in free energy ΔF due to the presence of the bubble, which is an essential ingredient for the nucleation rate Γ [see Eq. (21)]. ΔF can be calculated either directly from (2) or, in a computationally faster way, by using the formula

$$\Delta F(T) = \frac{4\pi}{3} R_c^3(T) \Delta p(T) + 4\pi\sigma(T) R_c^2(T). \qquad (37)$$

This expression resembles the thin-wall expression for ΔF, but here the temperature dependence of the surface tension makes this formula a good approximation to the exact value obtained using (2), once the functions $R_c(T)$, $\Delta p(T)$, and $\sigma(T)$ are known. The different results to ΔF, calculated using a simple thin-wall (where σ is a constant), using Eq. (37) (which we call *T-dependent thin-wall*), and from Eq. (2), are shown in Fig. 5. In our following computations, we use Eq. (37).

B. Time evolution

Now that we have all the necessary elements, we may investigate the time evolution of the system. We first analyze how the temperature evolves with time if we consider the reheating backreaction effects on the expanding system. As a first example, we consider three different expansion rates: $H^{-1} = 100$ fm/c (fast), $H^{-1} = 600$ fm/c (critical), and $H^{-1} = 10^7$ fm/c (slow). From Fig. 6 we can see that in the first case the temperature drops so fast that the system reaches the spinodal temperature without having time to grow enough bubbles to reheat. This is an example of a *quench* into the spinodal region. As the expansion rate H is lowered, the growing bubbles eventually have time to effectively release enough latent heat. Then, the cooling process is reversed and the temperature is raised to a value close to (and lower than) T_c. In this way the phase transition is completed through bubble nucleation. When the whole plasma is hadronized, there is no more release of latent heat, the expansion once again dominates, and the temperature falls abruptly. For the realistic equation of state we adopt, we find that the lowest (critical) expansion rate H at which there is reheating corresponds approximately to $H^{-1} = 600$ fm/c. Finally, we also consider a very low expansion and verify that the phase conversion proceeds almost entirely at $T = T_c$, which is equivalent to having an almost *in equilibrium*

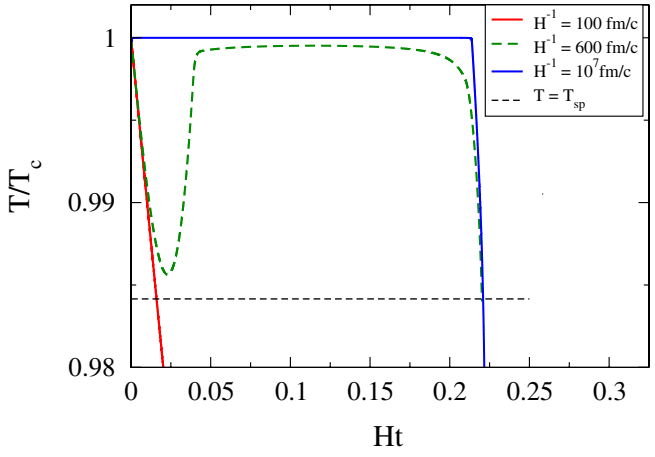

FIG. 6 (color online). Temperature, in units of T_c, as a function of time, in units of $1/H$, for different expansion rates.

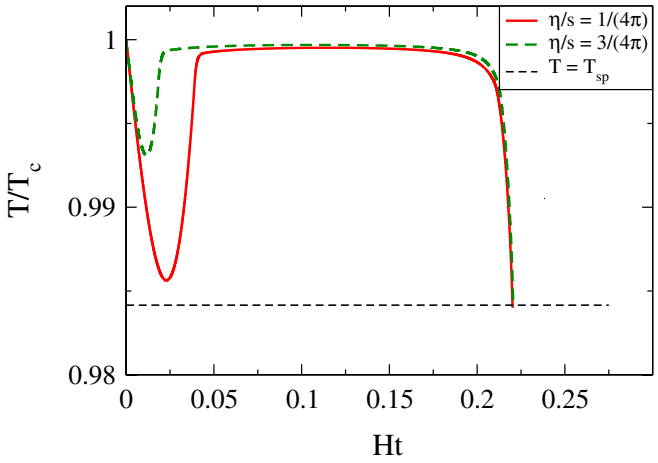

FIG. 8 (color online). Temperature, in units of T_c, as a function of time, in units of $1/H$ for different values of viscosity with $H^{-1} = 600$ fm$/c$.

phase conversion. Notice, however, that, if we take a closer look at the temperature as a function of time, even for the slowest expansion rate there is a slight supercooling in the beginning of the phase transition (as can be seen in the zoom for early times displayed in Fig. 7). In any case, the slower the expansion rate, the closer to equilibrium the transition evolves. Furthermore, the product $Ht_{\rm sp}$ is the same for all expansion rates.

Dissipation effects can generally affect significantly the dynamics of phase conversion, even in the case of an explosive spinodal decomposition [22]. In our framework, viscosity enters as a parameter in the dynamical prefactor of the nucleation rate [see Eq. (24)]. Recalling that the viscosity of the QGP is presumably very small [2,41] and that, on the other hand, holographic models set a lower bound ($\eta_{\rm AdS}/s = 1/4\pi$) [42], we compare the dynamics of the phase conversion for two values of viscosity: $\eta_{\rm AdS}$ and $3\eta_{\rm AdS}$. Figure 8 shows that by increasing the viscosity from $\eta_{\rm AdS}$ to $3\eta_{\rm AdS}$ the supercooling decreases approximately by a factor of 2, although the time to complete the transition remains unaffected.

The effects of different values of latent heat on the dynamics of the phase transition was also studied. In Fig. 9, we show the time evolution of the temperature considering the two equations of state discussed in Sec. II B and an expansion rate $H^{-1} = 600$ fm$/c$.

In Fig. 9 we can see that the EoS provided by the bag model, which leads to a latent heat larger than the one produced by the mixed EoS we adopt, implies a different transition dynamics. In fact, the larger latent heat of the bag EoS leads to a faster reheating of the plasma, since each nucleated bubble releases much more latent heat. Thus, a faster reheating means that the system will spend more time close to the critical temperature and the average nucleation rate will be much smaller for higher values of latent heat. Therefore, as can be seen in the figure, the nucleation process will take much longer to be completed.

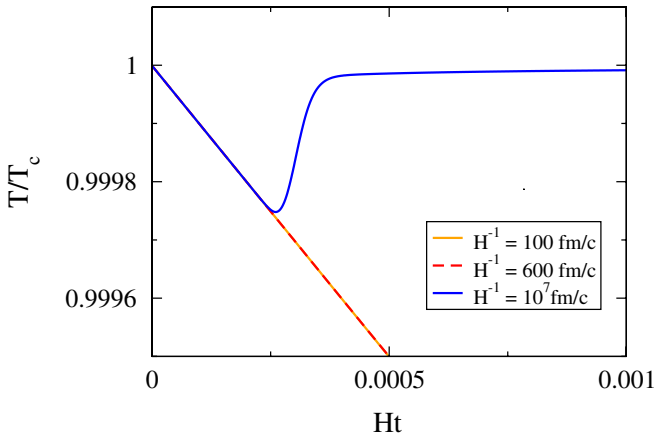

FIG. 7 (color online). Temperature, in units of T_c, as a function of time, in units of $1/H$, for different expansion rates at early times.

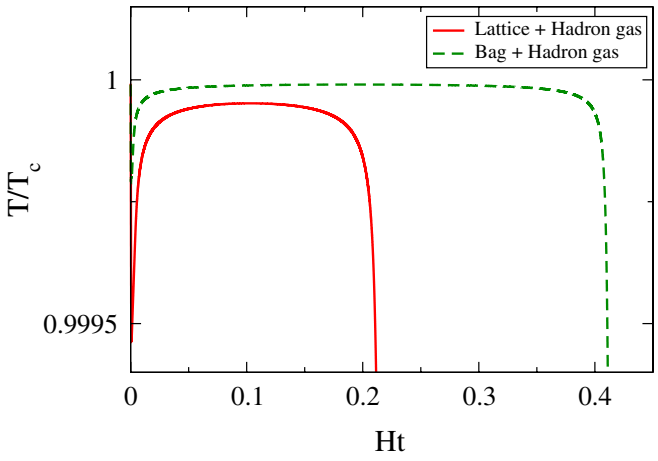

FIG. 9 (color online). Temperature, in units of T_c, as a function of time, in units of $1/H$, for the mixed and the bag model equations of state with $H^{-1} = 600$ fm$/c$.

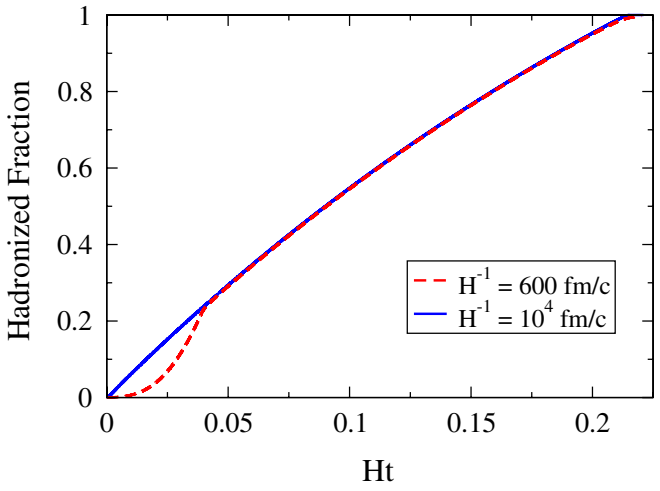

FIG. 10 (color online). Hadronized fraction of space as a function of time for $H^{-1} = 600$ fm$/c$ (critical expansion) and for $H^{-1} = 10^4$ fm$/c$ (slow expansion).

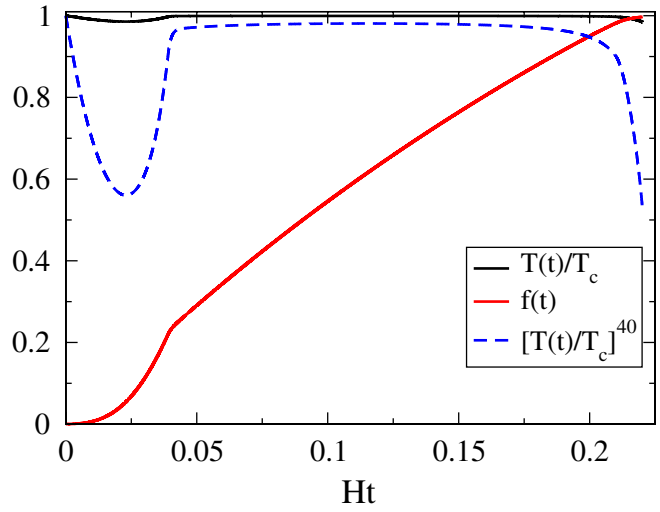

FIG. 11 (color online). $T(t)$ and $f(t)$ for $H^{-1} = 600$ fm$/c$. Full lines are the actual $T(t)$ and $f(t)$, and the dashed line is a *zoomed* $T(t)$ for comparison with $f(t)$.

We can now focus on the hadronic fraction of the plasma, i.e., the fraction which has been hadronized via bubble nucleation up to time t, $f(t)$. As can be easily seen from Eq. (32), $f(t)$ depends very strongly on $\tilde{\delta} \equiv 1 - T/T_c$, another measure of the supercooling. In fact, for a small $\tilde{\delta}$, when the thin-wall approximation is valid,

$$\Gamma(T) = \frac{\mathcal{P}_0}{2\pi} \exp[-\Delta F/T] \approx \frac{\mathcal{P}_0}{2\pi} \exp\left[-\frac{16\pi\sigma^3}{3\ell^2 T_c \tilde{\delta}^2}\right], \quad (38)$$

which depends very strongly on $\tilde{\delta}$. This implies that $f(t)$ will also grow exponentially as the temperature decreases, but before reheating effects are manifest. Indeed, after reheating the fluid temperature is near T_c and it is unlikely that new bubbles nucleate. This means that after reheating $f(t)$ grows due to the expansion of the existing bubbles, i.e. in a much milder fashion than during the supercooling phase, as can be seen in Fig. 10. We also notice that, for a slow expansion, the first stage (nucleation of new bubbles) takes place very early, and almost all of the dynamics of phase conversion is due to the expansion of the bubbles.

By examining both $T(t)$ and $f(t)$ on the same plot (Fig. 11), one can see quite clearly the relation between the reheating and the growth of $f(t)$ on one hand and, on the other hand, that after the reheating the temperature drops only after the phase transition is completed, i.e., after the system reaches $f = 1$.

If the plasma is quenched directly into the spinodal region and its hadronization begins, there will also be a release of latent heat, just like in nucleation, and the system may also reheat. A curious possibility is that of a double process phase conversion, in which the reheating takes the plasma back to some metastable temperature, in which nucleation dominates. As a result, part of the plasma is converted through spinodal decomposition and part by (inhomogeneous) nucleation. It would also be interesting to explore experimental consequences of such a hybrid transition process.

IV. CONCLUSIONS AND OUTLOOK

Using two different equations of state, a realistic matching of hadron gas of resonances and lattice QCD for $N_f = 2 + 1$ on one side, and the bag model (matched onto a hadron gas in the low temperature sector) on the other, we calculated both static and dynamical features of homogeneous bubble nucleation in a weakly first-order quark-hadron transition scenario, which is physically appealing if one takes into account results from the lattice and from experiments, as well as the nonequilibrium nature of the phase conversion process, especially in the case of high-energy heavy-ion collisions.

After setting up an effective potential, we obtained numerically bubble profiles, critical radii, the surface tension, and the free energy as functions of the temperature. We also compared our numerical results to those derived in the thin-wall approximation. We showed how this approximation (valid only near the critical temperature) can be used to *overestimate* the nucleation rate for lower temperatures. This indicates that an adequate approach to the dynamics of nucleation away from T_c should take into account exact bubble profiles $\phi(r)$, which in general have to be calculated numerically. With these *static* quantities we were able to feed a model for the dynamics of bubble nucleation in a homogeneously and isotropically expanding plasma, which is often adopted in studies of the early universe and heavy-ion collisions. Within this model, the only essential difference between these two physical settings is the value of the inverse Hubble constant H^{-1}, which is about 10^{19} fm$/c$ in the early Universe during the quark-hadron transition era, and about 10 fm$/c$ in the case

of heavy-ion experiments. We computed the temperature and the fraction of hadronized plasma as functions of time for different expansion rates, H, in order to make a quantitative estimate of the importance of nucleation in (homogeneous and isotropic) expanding systems.

In the scenario of a weakly first-order transition investigated in this paper, it is clear that nucleation remains as the dominant mechanism of phase conversion in the early universe, as expected from the standard cosmological picture. Nevertheless, previous estimates for relevant time scales using the bag model equation of state, which yields a much stronger first-order transition, may differ by a factor of 2 when compared to results from a more realistic equation of state. For high-energy heavy-ion collisions, where the plasma expands very quickly, the main mechanism for phase conversion must be greatly dominated by spinodal decomposition, which possibly has some effect on particle correlations and fluctuation [21,28–30,46–51]. This issue will be addressed in a future publication.

ACKNOWLEDGMENTS

The authors thank T. Kodama for fruitful discussions. E. S. F. is grateful to T. Mendes for many useful comments and discussions. This work was partially supported by CAPES, CNPq, FAPERJ, FAPESP, and FUJB/UFRJ.

[1] P. Steinberg *et al.*, J. Phys. G **34**, S173 (2007).
[2] B. Muller and J. L. Nagle, Annu. Rev. Nucl. Part. Sci. **56**, 93 (2006).
[3] E. W. Kolb and M. S. Turner, *The Early Universe* (Addison-Wesley, Redwood City, 1990).
[4] D. J. Schwarz, Ann. Phys. (Leipzig) **12**, 220 (2003); D. Boyanovsky, H. J. de Vega, and D. J. Schwarz, Annu. Rev. Nucl. Part. Sci. **56**, 441 (2006).
[5] E. Laermann and O. Philipsen, Annu. Rev. Nucl. Part. Sci. **53**, 163 (2003).
[6] Y. Aoki, Z. Fodor, S. D. Katz, and K. K. Szabo, Phys. Lett. B **643**, 46 (2006); M. Cheng *et al.*, Phys. Rev. D **77**, 014511 (2008); O. Philipsen, Prog. Theor. Phys. Suppl. **174**, 206 (2008).
[7] P. C. Hohenberg and B. I. Halperin, Rev. Mod. Phys. **49**, 435 (1977); G. Odor, Rev. Mod. Phys. **76**, 663 (2004).
[8] J. D. Gunton, M. San Miguel, and P. S. Sahni, in *Phase Transitions and Critical Phenomena*, edited by C. Domb and J. L. Lebowitz (Academic Press, London, 1983), Vol. 8; K. Binder, Rep. Prog. Phys. **50**, 783 (1987); J. S. Langer, in *Solids Far from Equilibrium*, edited by C. Godrèche (Cambridge University Press, Cambridge, England, 1992); N. Goldenfeld, *Lectures on Phase Transitions and the Renormalization Group* (Addison-Wesley, New York, 1992); A. J. Bray, Adv. Phys. **43**, 357 (1994).
[9] S. Caracciolo, A. Gambassi, M. Gubinelli, and A. Pelissetto, Phys. Rev. E **72**, 056111 (2005); W. G. Wanzeller, T. Mendes, and G. Krein, Phys. Rev. E **74**, 051123 (2006); T. Otobe and K. Okano, Int. J. Mod. Phys. C **17**, 1 (2006).
[10] B. A. Berg *et al.*, Nucl. Phys. B, Proc. Suppl. **129**, 587 (2004); Phys. Rev. D **69**, 034501 (2004); B. A. Berg, H. Meyer-Ortmanns, and A. Velytsky, Phys. Rev. D **70**, 054505 (2004); B. A. Berg, A. Velytsky, and H. Meyer-Ortmanns, Nucl. Phys. B, Proc. Suppl. **140**, 571 (2005); A. Bazavov, B. A. Berg, and A. Velytsky, Nucl. Phys. B, Proc. Suppl. **140**, 574 (2005); Int. J. Mod. Phys. A **20**, 3459 (2005); Phys. Rev. D **74**, 014501 (2006); A. Bazavov, B. A. Berg, and A. Dumitru, Phys. Rev. D **78**, 034024 (2008).
[11] K. Yagi, T. Hatsuda, and Y. Miake, Cambridge Monogr. Part. Phys., Nucl. Phys., Cosmol. **23**, 1 (2005).
[12] H. Reinhardt, B. V. Dang, and H. Schulz, Phys. Lett. **159B**, 161 (1985); H. Reinhardt and B. V. Dang, Phys. Lett. B **173**, 473 (1986).
[13] L. P. Csernai and J. I. Kapusta, Phys. Rev. D **46**, 1379 (1992).
[14] L. P. Csernai and J. I. Kapusta, Phys. Rev. Lett. **69**, 737 (1992).
[15] J. I. Kapusta, A. P. Vischer, and R. Venugopalan, Phys. Rev. C **51**, 901 (1995); J. I. Kapusta and A. P. Vischer, Phys. Rev. C **52**, 2725 (1995).
[16] T. Csorgo and L. P. Csernai, Phys. Lett. B **333**, 494 (1994); L. P. Csernai and I. N. Mishustin, Phys. Rev. Lett. **74**, 5005 (1995); I. N. Mishustin and O. Scavenius, Phys. Rev. Lett. **83**, 3134 (1999).
[17] E. E. Zabrodin, L. V. Bravina, L. P. Csernai, H. Stoecker, and W. Greiner, Phys. Lett. B **423**, 373 (1998); E. E. Zabrodin, L. Bravina, H. Stoecker, and W. Greiner, Phys. Rev. C **59**, 894 (1999).
[18] O. Scavenius and A. Dumitru, Phys. Rev. Lett. **83**, 4697 (1999).
[19] P. Shukla, A. K. Mohanty, S. K. Gupta, and M. Gleiser, Phys. Rev. C **62**, 054904 (2000); P. Shukla and A. K. Mohanty, Phys. Rev. C **64**, 054910 (2001).
[20] O. Scavenius, A. Dumitru, E. S. Fraga, J. T. Lenaghan, and A. D. Jackson, Phys. Rev. D **63**, 116003 (2001).
[21] A. Dumitru and R. D. Pisarski, Phys. Lett. B **504**, 282 (2001); Nucl. Phys. **A698**, 444 (2002); O. Scavenius, A. Dumitru, and A. D. Jackson, Phys. Rev. Lett. **87**, 182302 (2001).
[22] E. S. Fraga and G. Krein, Phys. Lett. B **614**, 181 (2005); E. S. Fraga, T. Kodama, G. Krein, A. J. Mizher, and L. F. Palhares, Nucl. Phys. **A785**, 138 (2007); E. S. Fraga, G. Krein, and A. J. Mizher, Phys. Rev. D **76**, 034501 (2007).
[23] K. Enqvist, J. Ignatius, K. Kajantie, and K. Rummukainen, Phys. Rev. D **45**, 3415 (1992); J. Ignatius, K. Kajantie, H. Kurki-Suonio, and M. Laine, Phys. Rev. D **49**, 3854 (1994); H. Kurki-Suonio and M. Laine, Phys. Rev. D **54**, 7163 (1996); J. Ignatius and D. J. Schwarz, Phys. Rev. Lett. **86**, 2216 (2001).

[24] A. Megevand and A. D. Sanchez, Phys. Rev. D **77**, 063519 (2008); A. Megevand, Phys. Rev. D **78**, 084003 (2008).
[25] M. Gell-Mann and M. Levy, Nuovo Cimento **16**, 705 (1960).
[26] S. P. Klevansky, Rev. Mod. Phys. **64**, 649 (1992).
[27] R. D. Pisarski, Phys. Rev. D **62**, 111501 (2000).
[28] K. Paech, H. Stoecker, and A. Dumitru, Phys. Rev. C **68**, 044907 (2003); K. Paech and A. Dumitru, Phys. Lett. B **623**, 200 (2005).
[29] C. E. Aguiar, E. S. Fraga, and T. Kodama, J. Phys. G **32**, 179 (2006); B. G. Taketani and E. S. Fraga, Phys. Rev. D **74**, 085013 (2006); A. Dumitru, L. Portugal, and D. Zschiesche, Phys. Rev. C **73**, 024902 (2006).
[30] C. Sasaki, B. Friman, and K. Redlich, Phys. Rev. Lett. **99**, 232301 (2007); Phys. Rev. D **77**, 034024 (2008).
[31] J. S. Langer, Ann. Phys. (N.Y.) **41**, 108 (1967); **281**, 941 (2000); **54**, 258 (1969); **65**, 53 (1971).
[32] J. S. Langer and L. A. Turski, Phys. Rev. A **8**, 3230 (1973); L. A. Turski and J. S. Langer, *ibid.* **22**, 2189 (1980).
[33] S. R. Coleman, Phys. Rev. D **15**, 2929 (1977); **16**, 1248(E) (1977); C. G. Callan and S. R. Coleman, Phys. Rev. D **16**, 1762 (1977).
[34] I. Affleck, Phys. Rev. Lett. **46**, 388 (1981).
[35] A. D. Linde, Phys. Lett. **100B**, 37 (1981); Nucl. Phys. **B216**, 421 (1983); **B223**, 544(E) (1983).
[36] M. Gleiser, G. C. Marques, and R. O. Ramos, Phys. Rev. D **48**, 1571 (1993).
[37] F. Karsch, K. Redlich, and A. Tawfik, Eur. Phys. J. C **29**, 549 (2003).
[38] T. Kodama (private communication).
[39] A. Bessa and E. S. Fraga, Rom. Rep. Phys. **58**, 087 (2006); B. W. Mintz, A. Bessa, and E. S. Fraga, arXiv:0810.2798.
[40] R. Venugopalan and A. P. Vischer, Phys. Rev. E **49**, 5849 (1994).
[41] B. Muller, Acta Phys. Pol. B **38**, 3705 (2007).
[42] P. Kovtun, D. T. Son, and A. O. Starinets, J. High Energy Phys. 10 (2003) 064.
[43] T. Csorgo and A. Ster, Heavy Ion Phys. **17**, 295 (2003).
[44] A. H. Guth and E. J. Weinberg, Phys. Rev. D **23**, 876 (1981).
[45] E. S. Fraga and R. Venugopalan, Physica (Amsterdam) **345A**, 121 (2004).
[46] I. N. Mishustin, Phys. Rev. Lett. **82**, 4779 (1999).
[47] H. Heiselberg and A. D. Jackson, Phys. Rev. C **63**, 064904 (2001).
[48] D. Bower and S. Gavin, Phys. Rev. C **64**, 051902 (2001).
[49] C. Pruneau, S. Gavin, and S. Voloshin, Phys. Rev. C **66**, 044904 (2002).
[50] P. Chomaz, M. Colonna, and J. Randrup, Phys. Rep. **389**, 263 (2004); J. Randrup, Phys. Rev. Lett. **92**, 122301 (2004); V. Koch, A. Majumder, and J. Randrup, Phys. Rev. C **72**, 064903 (2005).
[51] I. N. Mishustin, Proc. Sci., CPOD07 (2007) 010; B. Tomasik, I. Melo, G. Torrieri, I. Mishustin, P. Bartos, M. Gintner, and S. Korony, Acta Phys. Polon. Supp. **1**, 513 (2008).